MIXED CONVECTION OF FUNCTIONALIZED DWCNT-WATER NANOFLUID IN BAFFLED LID-DRIVEN CAVITIES

by

Mohammad HEMMAT ESFE[a*], Ali Akbar ABBASIAN ARANI[b], Wei-Mon YAN[c*], Alireza AGHAIE[b], Masoud AFRAND[a], and Nima SINA[a]

[a] Department of Mechanical Engineering, Najafabad Branch, Islamic Azad University, Isfahan, Iran
[b] Department of Mechanical Engineering, University of Kashan, Kashan, Iran
[c] Department of Energy and Refrigerating Air-Conditioning Engineering, National Taipei University of Technology, Taipei, Taiwan, ROC

Original scientific paper
https://doi.org/10.2298/TSCI160225216E

The present study aims to evaluate the mixed convection flow and heat transfer of functionalized DWCNT/water nanofluids with variable properties in a cavity having hot baffles. The investigation is performed at different nanoparticles volume fraction including 0, 0.0002, 0.001, 0.002, and 0.004, Richardson numbers ranging from 0.01 to 100, inclination angles ranging from 0 to 60° and at constant Grashof number of 10^4. The results presented as streamlines and isotherms plot and Nusselt number diagrams. According to the finding with increasing nanoparticles volume fraction and distance between the left hot baffles of nanoparticles average Nusselt number enhances for all considered Richardson numbers and cavity inclination angles. Also with increasing Richardson number, the rate of changes of average Nusselt number increase with increasing distance between the left hot baffles. For example, at Richardson number of 0.01, by increasing L_1 from 0.4 to 0.6, the average Nusselt number increases 7%; while for similar situation at Richardson number of 0.1, 1.0, and 10, the average Nusselt number increases, respectively, 17%, 24%, and 26%. At all Richardson numbers, the maximum value of average Nusselt number is achieved for a minimum length of left baffles.

Key words: *nanofluid, square cavity, baffle, functionalized DWCNT-water, mixed convection*

Introduction

Convection heat transfer with nanofluids is always encountered in many engineering applications such as solar collectors, heat exchangers, and cooling of electrical components [1-3]. In these applications, engineers are always looking for techniques to enhance the heat transfer performance using solid nanoparticles (less than 100 nm) in the common fluid (*e. g.* water, ethylene glycol, and oil). Due to the fact that the experimental investigation of heat transfer is costly and time-consuming process, numerical simulation has attracted the interest of researchers in recent decades to make available close comprehension to the heat transfer phenomenon. Since, applications of mixed convection heat transfer in cavities is very important, mixed convection in lid-driven cavities filled with nanofluids is one of the most interesting topics usually considered by researches.

* Corresponding author, e-mail: m.hemmatesfe@gmail.com or wmyan@ntut.edu.tw

Mixed convection in a square lid-driven cavity with copper-water nanofluid was executed numerically by Talebi *et al.* [4]. In their study, the top and bottom horizontal walls are insulated while the vertical walls are maintained at constant but different temperatures. The predicted results indicated that at fixed Reynolds number, the solid concentration of nanoparticles affects the flow pattern and thermal behavior particularly for a higher Rayleigh number. Also the results of this paper indicate the Nusselt number increase with increasing nanoparticles volume fraction. Mansour *et al.* [5] examined numerically mixed convection in a square lid-driven cavity partially heated from below and filled with water-based nanofluid containing various nanoparticles volume fractions of Cu, Ag, Al_2O_3, and TiO_2. The effects of Reynolds number, nanoparticles volume fraction, different values of the heat source length and different locations of the heat source on the Nusselt number were considered in details. The mixed convection in a lid-driven triangular enclosure filled with a Al_2O_3-water nanofluid was also examined numerically by Ghasemia and Aminossadati [6]. The results presented a comparison between two different scenarios of upward and downward left sliding walls and showed the addition of Al_2O_3 nanoparticles enhances the heat transfer rate for all values of Richardson number and for each direction of the sliding wall motion. Abbasian Arani *et al.* [7] predicted mixed convection flow of Cu-water nanofluid in a lid-driven square cavity with adiabatic horizontal walls and sinusoidal heating on sidewalls. The predicted results revealed that for a constant Grashof number at all Richardson numbers, a clockwise eddy was developed inside the cavity, also the rate of heat transfer increases with decrease in Richardson number and increase of nanoparticles volume fraction. Furthermore the results show for a constant Reynolds number the clockwise eddy is observed up to Ri = 1. For Ri = 10 a multicellular flow pattern is formed inside the cavity. The mixed convection in a square lid-driven cavity with filled with nanofluids was examined by Salari *et al.* [8]. The effects of the Rayleigh number, Reynolds number, the nanoparticles volume fraction, the dimensions of heaters, and their locations on the streamlines and isotherms contours were investigated in details. The results mentioned above focused on the constant thermophysical properties. But, in real applications, the effects of variable thermophysical properties in lid-driven cavity with nanofluids are important.

Here, a brief review of recent studies on mixed convection in lid-driven cavities using nanofluids considering variable properties was conducted. Numerical modeling of laminar mixed convection in single and double-lid square cavities filled with a Al_2O_3-water nanofluid was performed by Chamkha and Abu-Nada [9]. In their study, two viscosity models are used to approximate nanofluid viscosity, namely, the Brinkman model and the Pak and Cho correlation. Sheikhzadeh *et al.* [10] performed numerical study on mixed convection in a lid-driven square cavity containing Al_2O_3-water nanofluid focusing variable properties. They estimated the thermal conductivity and viscosity of nanofluid using the experimental models. The results obtained by variable thermal conductivity and viscosity were compared to the results obtained using the Maxwell and Brinkman model. Major differences were found between the heat transfer rates in the cavity for two employed models. Mixed convection of nanofluid consists of CuO and water inside a lid-driven cavity with wavy wall was numerically modeled by Abu-Nada and Chamkha [11]. Computational results revealed that heat transfer enhanced by adding the nanoparticles for all Richardson numbers and bottom wall geometry ratios. Also the presence of nanoparticles causes significant heat transfer augmentation for all values of Richardson numbers and bottom wall geometry ratios.

Modeling of flow and heat transfer in lid-driven cavity with obstacles and heat sources is another topic that has been considered recently [12-16]. The numerical solution of mixed convection flow in a lid-driven square enclosure with a triangular heat source filled with nanofluid is performed by Kalteh *et al.* [15]. The fluid in the enclosure was a water-based nanofluid containing Al_2O_3, TiO_2, Ag, or CuO nanoparticles. They presented that adding the nanoparticles in pure fluid leads to a noteworthy heat transfer enhancement. Hemmat Esfe *et al.* [16] numerically studied mixed convection in an inclined lid-driven cavity equipped to a hot obstacle using Al_2O_3/water nanofluid considering temperature-dependent properties. Aghaei *et. al.* [17] investigated the numerical study of magnetic field effect on mixed convection and entropy generation of nanofluid in a trapezoidal enclosure. For all of the studied cases, entropy generation due to friction is negligible and the total entropy generation is mainly due to irreversibility associated with heat transfer and variation of the total entropy generation with Hartmann number is similar to that of the average Nusselt number. Mixed convection heat transfer in a CuO–water filled trapezoidal enclosure, effects of various constant and variable properties of the nanofluid was numerically modeled by Arefmanesh *et. al.* [18]. The results indicated that the differences between the average Nusselt number and the entropy generation obtained using the different considered variable-property models decrease with increasing the nanoparticles volume fraction.

Mixed convection of water-based nanofluids in a rectangular inclined lid-driven cavity partially heated from its left side wall was investigated numerically by Hussein *et al.* [19] The results of this study indicate that the presence of nanoparticles in the fluid is found to alter the structure of the fluid flow. Moreover, it is observed that the shape of the circulation vortex is sensitive to the inclination angle and addition of nanofluids. Ahmed *et al.* [20] investigated numerically the mixed convection from a discrete heat source in enclosures with two adjacent moving walls and filled with micropolar nanofluids. Based on the numerical results, the effects of the dominant parameters such as Richardson number, nanofluid type, length and location of the heat source, nanoparticles volume fractions, moving lid orientations and dimensionless viscosity are examined.

Based on the best knowledge of author there is no study on mixed convection in cavity subjected to functionalized double-walled carbon nanotube-water (DWCNT-water) nanofluid. Furthermore, the effects of changing position of three baffles on control of heat transfer and fluid flow of cavity is considered in the present study.

Analysis

Problem formulation

The 2-D steady-state, laminar, mixed-convection fluid flow and heat transfer within a square enclosure filled with functionalized DWCNT-water nanofluid is simulated numerically using the finite volume method. The schematic of the present study is depicted in fig. 1. The dimensions of the enclosure are denoted by *H*. The top wall of the cavity moves in its own plane from left to right with a constant speed U_0. Left heated baffles have equal length at all cases and are kept at high temperature, T_h. Right hot baffle is located at middle of right wall.

In order to cast the governing equations into a dimensionless form, the following dimensionless variables are introduced:

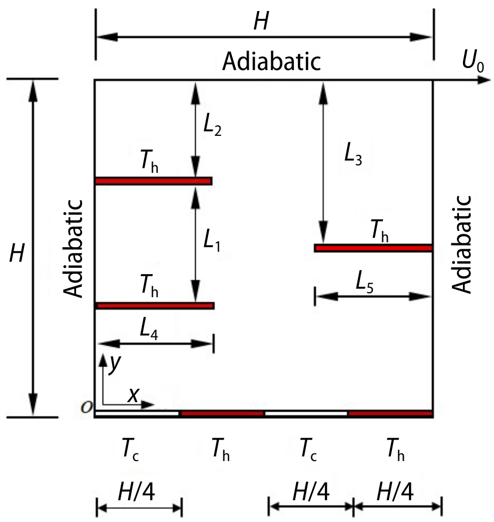

Figure 1. Schematic diagram of cavity with hot baffles

$$X=\frac{x}{H},\ Y=\frac{y}{H},\ U=\frac{u}{U_0},\ V=\frac{v}{U_0},\ P=\frac{p}{\rho_\mathrm{f}U_0^2},\ \theta=\frac{T-T_\mathrm{c}}{T_\mathrm{h}-T_\mathrm{c}} \tag{1}$$

Employing the foregoing dimensionless variable, the continuity, momentum, and energy equations for the nanofluid in a dimensionless form:

$$\frac{\partial U}{\partial X}+\frac{\partial V}{\partial Y}=0 \tag{2}$$

$$U\frac{\partial U}{\partial X}+V\frac{\partial U}{\partial Y}=-\frac{\partial P}{\partial X}+\frac{1}{\rho_\mathrm{nf}\nu_\mathrm{f}\,\mathrm{Re}}\left[\frac{\partial}{\partial X}\left(\mu_\mathrm{nf}\frac{\partial U}{\partial X}\right)+\frac{\partial}{\partial Y}\left(\mu_\mathrm{nf}\frac{\partial U}{\partial Y}\right)\right]+\frac{(\rho\beta)_\mathrm{nf}}{\rho_\mathrm{nf}\beta_\mathrm{f}}\mathrm{Ri}\,\theta\sin(\gamma) \tag{3}$$

$$U\frac{\partial V}{\partial X}+V\frac{\partial V}{\partial Y}=-\frac{\partial P}{\partial Y}+\frac{1}{\rho_\mathrm{nf}\nu_\mathrm{f}\,\mathrm{Re}}\left[\frac{\partial}{\partial X}\left(\mu_\mathrm{nf}\frac{\partial V}{\partial X}\right)+\frac{\partial}{\partial Y}\left(\mu_\mathrm{nf}\frac{\partial V}{\partial Y}\right)\right]+\frac{(\rho\beta)_\mathrm{nf}}{\rho_\mathrm{nf}\beta_\mathrm{f}}\mathrm{Ri}\,\theta\cos(\gamma) \tag{4}$$

$$U\frac{\partial \theta}{\partial X}+V\frac{\partial \theta}{\partial Y}=\frac{1}{\mathrm{Re}\,\mathrm{Pr}\,\alpha_\mathrm{f}(\rho c_p)_\mathrm{nf}}\left[\frac{\partial}{\partial X}\left(k_\mathrm{nf}\frac{\partial \theta}{\partial X}\right)+\frac{\partial}{\partial Y}\left(k_\mathrm{nf}\frac{\partial \theta}{\partial Y}\right)\right] \tag{5}$$

where γ is the cavity inclination angle.

The dimensionless boundary conditions are given:

$$\begin{gathered}
0<X<H,\quad Y=1,\quad U=1,\quad V=0,\quad \text{and}\quad \frac{\partial\theta}{\partial n}=0\\
0<Y<H,\quad X=0,\quad U=0,\quad V=0,\quad \text{and}\quad \frac{\partial\theta}{\partial n}=0\\
0<Y<H,\quad X=1,\quad U=0,\quad V=0,\quad \text{and}\quad \frac{\partial\theta}{\partial n}=0\\
X=0,\quad 0<y<H,\quad U=0,\quad V=0\\
X=0,\quad 0<y<\frac{H}{4},\quad \theta=0-\frac{H}{4}<y<\frac{H}{2},\quad \theta=1-\frac{H}{2}<y<\frac{3H}{4},\\
\theta=0-\frac{3H}{4}<y<H,\quad \theta=1\\
\text{On all baffle,}\quad \theta=1
\end{gathered} \tag{6}$$

The local Nusselt number is obtained from the relation:

$$\mathrm{Nu}=-\left(\frac{k_\mathrm{nf}}{k_\mathrm{f}}\right)\frac{\partial\theta}{\partial n}\bigg|_\text{on all hot sections} \tag{7}$$

The average Nusselt number is given:

$$\mathrm{Nu}_\mathrm{Avg}=\frac{1}{L_\text{on all hot sections}}\int \mathrm{Nu}\,\mathrm{d}Y \tag{8}$$

In order to investigate the effect of the thermal conductivity and viscosity of the nanofluid, experimental results [21] are employed for DWCNT-water nanofluid in the present study:

$$\frac{k_\mathrm{nf}}{k_\mathrm{f}}=\frac{\varphi}{0.17981-0.000369T}+1.0026 \tag{9}$$

$$\frac{\mu_{\mathrm{nf}}}{\mu_{\mathrm{f}}}=1+3.575\varphi+6032.93\varphi^2-1153669\varphi^3 \tag{10}$$

Numerical implementation

The finite volume method and the SIMPLER algorithm are employed to solve the governing equations numerically. The first step of discretizing the governing equations is to generate a finite difference mesh in the computational domain. A control volume is generated around each node of the mesh afterwards. The governing equations are then integrated over each control volume. The diffusion terms are replaced using a second-order central difference scheme, while, a hybrid scheme is employed for the convective terms in order to obtain stable solutions for convection-dominated cases.

Validation of the code

In order to validate the numerical procedure, the mixed-convection fluid flow and heat transfer in a square cavity filled with Al_2O_3-water nanofluid is simulated using the developed code, and the results are compared with the existing results in the literature. The cavity is filled with Al_2O_3-water nanofluid. Table 1 shows comparisons between the average Nusselt number of the hot wall obtained by the present code with the results of Chamkha and Abu-Nada [9]. As it is observed from the table, very good agreements exist between the results of the present simulation.

Table 1. Comparisons between the average Nusselt number of the hot wall with the results of Chamkha and Abu-Nada [9]

Ri	φ	Nu_{Avg}		
		Present work	Chamkha and Abu-Nada [9]	Percent difference
0.01	0.02	33.14	32.80	1.04
	0.1	36.40	36.90	1.36
1	0.02	4.76	4.92	3.25
	0.1	4	4.95	2.22

3.2 Grid independence study

In order to determine a proper grid for the numerical simulations, a grid independence study is carried out. The obtained average Nusselt number of the hot wall for these grids are presented in tab. 2.

It is observed from this table that the average Nusselt number converges for a grid having 131×131 nodes implying that this grid is sufficiently The convergence criterion in the following numerical simulations for the temperature, pressure, and velocity fields is:

$$\frac{\sum_{i=1}^{M}\sum_{j=1}^{N}\left|\xi_{i,j}^{r+1}-\xi_{i,j}^{r}\right|}{\sum_{i=1}^{M}\sum_{j=1}^{N}\left|\xi_{i,j}^{r+1}\right|}\le 10^{-7} \tag{11}$$

Table 2. The average Nusselt number of φ = 0.004 and Ri = 1, γ = 0

Number of grid points	Nu_{avg}
71×71	1.157
91×91	1.166
111×111	1.174
131×131	1.176
151×151	1.777

where *m* and *n* are the number of grid points in the x- and y-directions, respectively, ξ is any of the computed field variables, and *r* is the number of iterations.

Results and discussion

In this work, mixed convection flow and heat transfer of square cavity subjected to DWCNT-water nanofluids with variable properties having three hot baffles was numerically studied. The study was performed at constant Grashof number of 10^4, for different Richardson numbers ranging from 0.01 to 100, inclination angles ranging from 0 to 60° and for different nanoparticles volume fractions (0, 0.0002, 0.001, 0.002, and 0.004).

Figure 2 shows the streamlines and isotherms of COOH-functionalized DWCNT-water for different inclination angles and Richardson numbers at nanoparticles volume fraction of 0.004. At inclination angle of 0 (Case 1) and for all Richardson numbers, a great vortex occurs in the upper part of the enclosure near the moving wall. At all Richardson number, streamlines are more compact in the vicinity of moving wall. This behavior of streamlines is due to the fact that this vortex is strongly affected by the velocity of moving wall. Also, for all Richardson numbers the center of the vortex, proportional to the speed of the wall, is leaning to the right

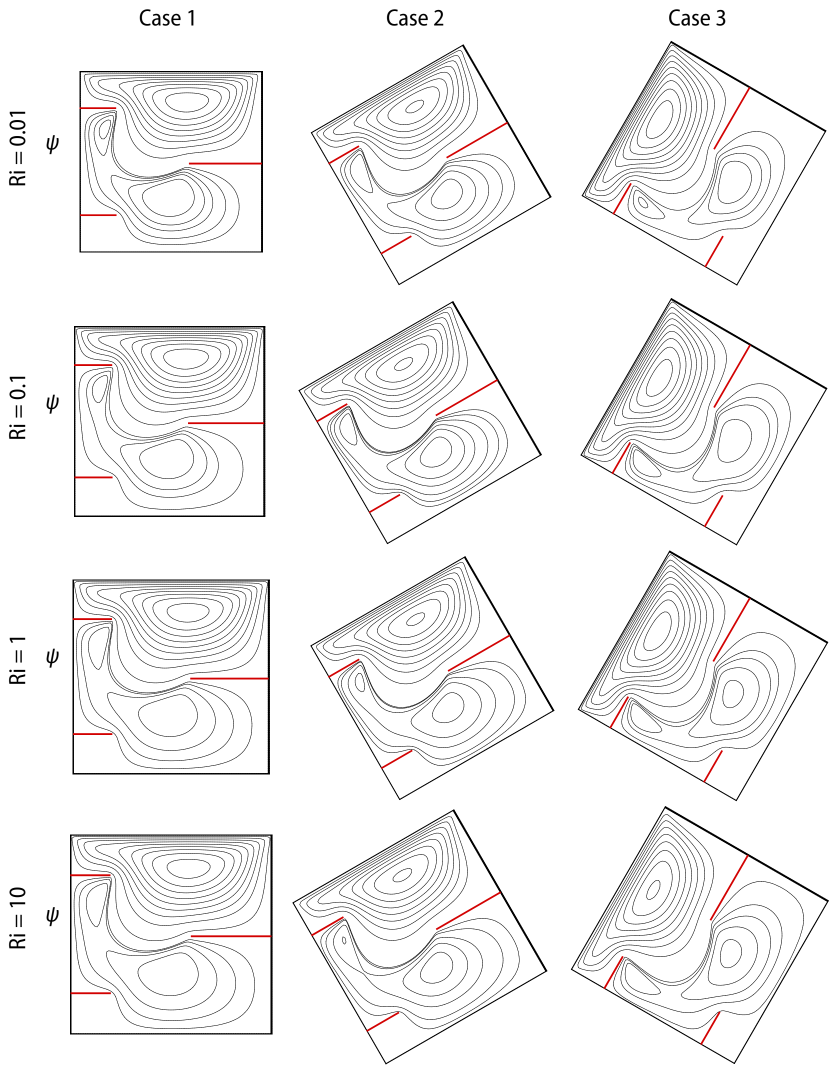

Figure 2(a). Streamlines of COOH-functionalized DWCNT-water at different inclination angles and Richardson numbers at nanoparticles volume fraction of 0.004

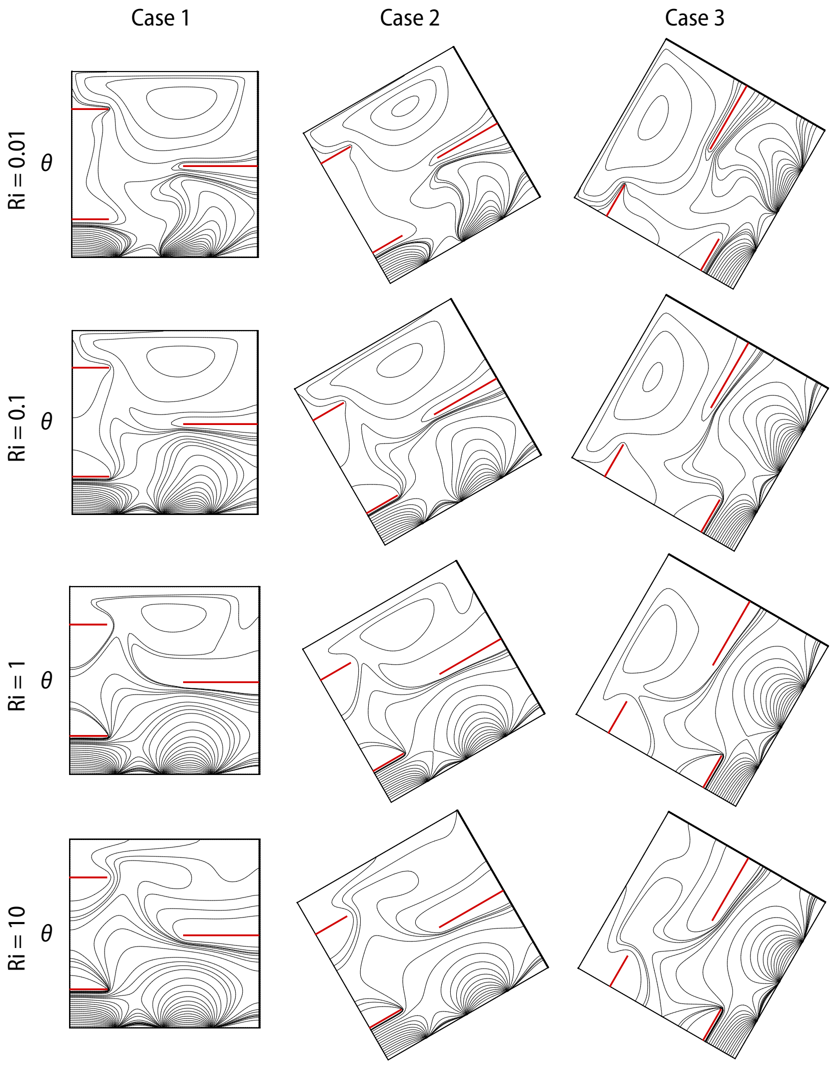

Figure 2(b). Isotherms of COOH-functionalized DWCNT-water at different inclination angles and Richardson numbers at nanoparticles volume fraction of 0.004

side of the enclosure. At Richardson number of 0.01, the slope of the streamlines in the upper right corner of the enclosure is higher compared to other Richardson numbers, which is due to higher velocity of moving wall at Richardson number of 0.01. In the Case 1, secondary vortex forms in the lower section of enclosure under the influence of hot baffles and lower hot parts. At central zone of secondary vortex, under the influence of the vortex formed in the upper part of the enclosure, streamlines is more compact. By changing the inclination angle of enclosure, there is not a significant change in the overall behavior of flow. At inclination angles of 30° and 60° (Case 2 and Case 3), for all Richardson numbers, two vortexes are observed. In these cases, because of the buoyancy force components, the upper large vortex is slightly affected by direction of moving wall velocity. By comparing the slope of the streamlines in the upper right corner, at Richardson number of 0.01 and for different inclination angles of enclosure, this phenomenon is characterized clearly. With increasing the inclination angle, the secondary vortex in the lower section of enclosure tends to the left and its distance from the adiabatic left wall of the enclosure increases. For all cases, isotherms in the vicinity of the lower wall of enclosure are denser which is due to the higher rate of heat transfer in this part of the enclosure. In the lower right side zone, isotherms, with high curvature, are stretched towards the right adiabatic wall which decreased with increasing Richardson number. Greater curvature of the isotherms in the whole of enclosure, at the small Richardson numbers, indicates greater movement of nanofluids at these Richardson numbers. With increasing the Richardson number isotherms tend to a thermal stratification, however, due to the hot baffle at different parts of the enclosure thermal stratification is not well formed.

Maximum amount of stream function Ψ_{max} as a criterion of the flow power, in various Richardson numbers for nanofluid with nanoparticles volume fraction of $\varphi = 0.004$ is presented in tab. 3. In all γ with increasing Richardson numbers the value of the Maximum of stream function decrease.

Table 3. Amounts of Ψ_{max} in all Richardson number and for nanofluid in $\varphi = 0.004$

Ri	$\gamma = 0°$	$\gamma = 30°$	$\gamma = 60°$
0.01	$1.986 \cdot 10^{-3}$	$1.731 \cdot 10^{-3}$	$1.655 \cdot 10^{-3}$
0.1	$1.874 \cdot 10^{-3}$	$1.688 \cdot 10^{-3}$	$1.579 \cdot 10^{-3}$
1	$1.763 \cdot 10^{-3}$	$1.565 \cdot 10^{-3}$	$1.497 \cdot 10^{-3}$
10	$1.544 \cdot 10^{-3}$	$1.432 \cdot 10^{-3}$	$1.324 \cdot 10^{-3}$

Figure 3 demonstrates the variation of average Nusselt number versus nanoparticles volume fraction at different Richardson numbers for different distances, L_1,) between the left hot

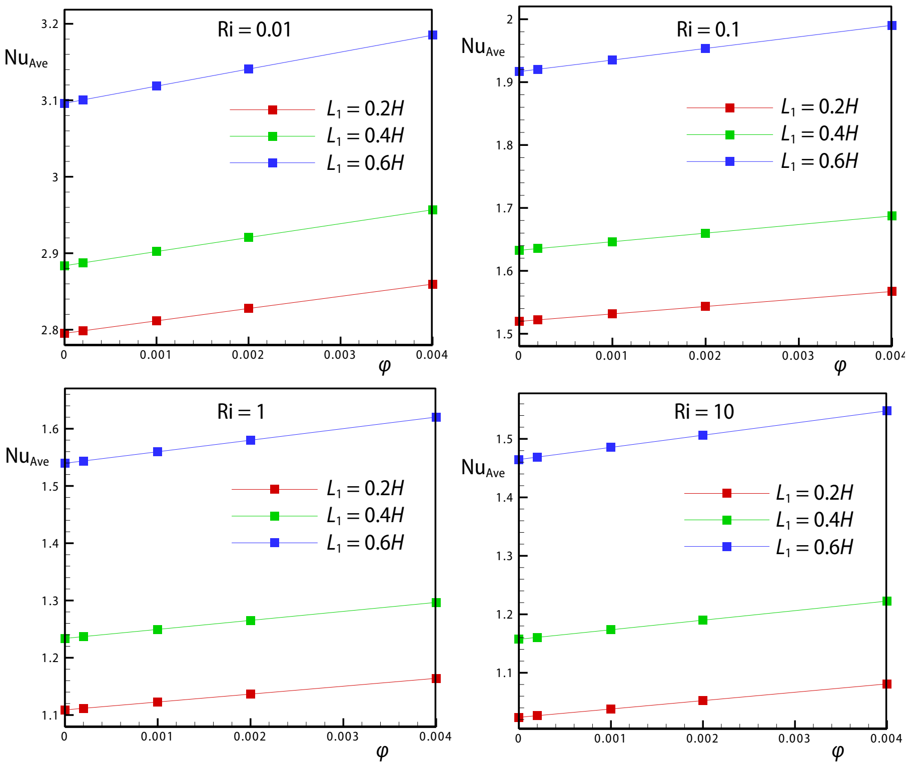

Figure 3. The variation of average Nusselt number *vs.* nanoparticles volume fraction at different Richardson numbers at different (L_1) between the left hot baffles

baffles. For all L_1 at all Richardson numbers, with increasing nanoparticles volume fraction average Nusselt number enhances. For all cases at all Richardson numbers, with increasing L_1 average Nusselt number increases and better temperature distribution occurs throughout the enclosure. Increase in L_1 also provides more space to move nanofluids, which leads to improve heat transfer rate. With increase in Richardson number, the values of average Nusselt number decrease compared with the similar conditions for lower Richardson numbers. When the Richardson number increases, the amounts of changes of average Nusselt number increase with increasing L_1. For example, at Ri = 0.01, by increasing L_1 from 0.4 of height of enclosure to 0.6 of it, the average Nusselt number increases 7%; while for similar situation at Richardson number of 0.1, 1.0, and 10, the average Nusselt number increases, respectively, 17%, 24%, and 26%. Obtained results are similar with previous research in view to baffles locations [22-24] and lid velocity, changing the Richardson number [5, 25, 26].

The variation of average Nusselt number *vs.* nanoparticles volume fraction at different Richardson numbers for different lengths, L_4,) of the left hot baffles is illustrated in fig. 4. For all L_4 at all Richardson numbers, with increasing nanoparticles volume fraction average Nusselt number enhances. For all cases considered, with increasing Richardson number, the variation of average Nusselt number with the nanoparticles volume fraction is more perceptible. At all Richardson numbers, the maximum value of average Nusselt number is achieved for a minimum length of left baffles. For conditions considered in fig. 3, at low Richardson numbers, the values of average Nusselt number are greater than similar

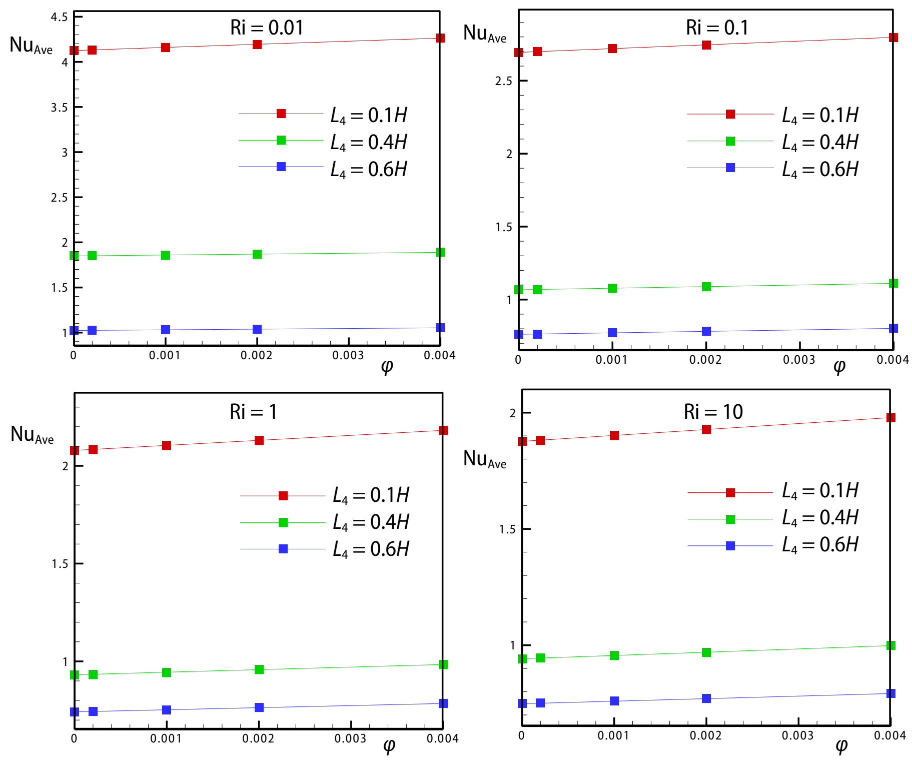

Figure 4. The variation of average Nusselt number *vs.* nanoparticles volume fraction at different Richardson numbers for different lengths (L_4) of the left hot baffles

situations at high Richardson numbers. Obtained results in this section also are similar with previous research in view to baffles locations [22-24] and lid velocity, changing the Richardson number [5, 25, 26].

In eq. (9) the new correlation is proposed to predict the average Nusselt number for $\gamma = 0°$ to $\gamma = 60°$.

$$\begin{gathered}\mathrm{Nu} = A\,\mathrm{Ri}^3 + B\,\mathrm{Ri}^2 + C\,\mathrm{Ri} + D\varphi + E \\ A = -1.3, \quad B = 14.53, \quad C = -14.92, \quad D = 14.52, \quad E = 2.82, \quad R^2 = 0.999\end{gathered} \tag{9}$$

Conclusions

In this study, mixed convection flow and heat transfer of DWCNT-water nanofluid with variable properties in an enclosure equipped with hot baffles was numerically investigated. The study was conducted at Grashof number of 10^4, for Richardson numbers ranging from 0.01 to 100, inclination angles ranging from 0 to 60° and for different nanoparticles volume fractions (0, 0.0002, 0.001, 0.002, and 0.004). Also, the effect of length and location of hot baffles on fluid flow and heat transfer were investigated. Based on the numerical results, the following conclusions were obtained.

- For all considered Richardson numbers and inclination angles, with increasing nanoparticles volume fraction average Nusselt number enhances.
- For all cases at all Richardson numbers, with increasing distance between the left hot baffles average Nusselt number increases.
- With increasing Richardson number, the amounts of changes of average Nusselt number increase with increasing distance between the left hot baffles. For example, at Richardson number of 0.01, by increasing L_1 from 0.4 to 0.6, the average Nusselt number increases 7%; while for similar situations at Richardson number of 0.1, 1.0, and 10, the average Nusselt number increases 17%, 24%, and 26%, respectively.
- At all Richardson numbers, the maximum value of average Nusselt number is achieved for a minimum length of left baffles.

Acknowledgment

The financial support by the Ministry of Science and Technology, ROC, through the contract MOST 103-2221-E-027 -107-MY2 is highly appreciated.

Nomenclature

g – gravitational acceleration, [ms^{-2}]
h – heat transfer coefficient, [Wm^{-2}K^{-1}]
k – thermal conductivity, [Wm^{-1}K^{-1}]
L – enclosure length, [m]
Nu – Nusselt number, [–]
P – dimensionless pressure, [–]
Pr – Prandtl number, [–]
Ri – Richardson number, [–]
T – temperature, [K]
U, V – dimensionless velocity components, [–]
X, Y – dimensionless Cartesian co-ordinates, [–]

Greek symbols

φ – nanoparticles volume fraction
θ – inclination angle of cavity, [°]
ψ – streamlines

Subscript

Avg – average
c – low temperature
f – fluid
h – high temperature
nf – nanofluid
p – nanoparticles

References

[1] Haddad, Z., *et al*., A Review on Natural Convective Heat Transfer of Nanofluids, *Renewable and Sustainable Energy Reviews, 16* (2012), 7, pp. 5363-5378

[2] Huminic, G., Huminic, A., Application of Nanofluids in Heat Exchangers: A Review, *Renewable and Sustainable Energy Reviews, 16* (2012), 8, pp. 5625-5638

[3] Mohammed, A. H., *et al*., Heat Transfer and Fluid Flow Characteristics in Microchannels Heat Exchanger Using Nanofluids: A Review, *Renewable and Sustainable Energy Reviews, 15* (2011), 3, pp. 1502-1512

[4] Talebi, F., *et al*., Numerical Study of Mixed Convection Flows in a Square Lid-Driven Cavity Utilizing Nanofluid, *International Communication in Heat and Mass Transfer, 37* (2010), 1, pp. 79-90

[5] Mansour, M. A., *et al*., Numerical Simulation of Mixed Convection Flows in a Square Lid-Driven Cavity Partially Heated from below Using Nanofluid, *International Communication in Heat and Mass Transfer, 37* (2010), 10, pp. 1504-1512

[6] Ghasemia, B., Aminossadati, S. M., Mixed Convection in a Lid-Driven Triangular Enclosure Filled with Nanofluids, *International Communication in Heat and Mass Transfer, 37* (2010), 8, pp. 1142-1148

[7] Abbasian Arani, A. A., *et al*., Numerical Study of Mixed Convection Flow in a Lid-Driven Cavity with Sinusoidal Heating on Sidewalls Using Nanofluid, *Superlattices and Microstructures, 51* (2012), 6, pp. 893-911

[8] Salari, M., *et al*., Mixed Convection of Nanofluid Flows in a Square Lid-Driven Cavity Heated Partially from Both the Bottom and Side Walls, *Numerical Heat Transfer, Part A, 62* (2012), 2, pp. 158-177

[9] Chamkha, A. J., Abu-Nada, E., Mixed Convection Flow in Single- and Double-Lid Driven Square Cavities Filled with water-Al_2O_3 Nanofluid: Effect of Viscosity Models, *European Journal of Mechanics B/ Fluids, 36* (2012), Nov.-Dec., pp.82-96

[10] Sheikhzadeh, G. A., *et al*., Numerical Study of Mixed Convection Flows in a Lid-Driven Enclosure Filled with Nanofluid Using Variable Properties, *Results in Physics, 2* (2012), Feb., pp. 5-13

[11] Abu-Nada, E., Chamkha, A. J., Mixed Convection Flow of a Nanofluid in a Lid-Driven Cavity with a Wavy Wall, *International Communications in Heat and Mass Transfer, 57* (2014), Oct., pp. 36-47

[12] Sun, C., *et al*., Control of Mixed Convection in Lid-Driven Enclosures Using Conductive Triangular Fins, *International Journal of Heat and Mass Transfer, 54* (2011), 4, pp. 894-909

[13] Hemmat Esfe, M., *et al*., Numerical Simulation of Natural Convection around an Obstacle Placed in an Enclosure Filled with Different Types of Nanofluids, *Heat Transfer Res., 45* (2014), 3, pp. 279-292

[14] Ray, S., Chatterjee, D., MHD Mixed Convection in a Lid-Driven Cavity Including Heat Conducting Circular Solid Object and Corner Heaters with Joule Heating, *International Communications in Heat and Mass Transfer, 57* (2014), Oct., pp. 200-207

[15] Kalteh, M., *et al*., Numerical Solution of Nanofluid Mixed Convection Heat Transfer in a Lid-Driven Square Cavity with a Triangular Heat Source, *Powder Technology, 253* (2014), Feb., pp. 780-788

[16] Hemmat Esfe, M., *et al*., Mixed-Convection Flow and Heat Transfer in an Inclined Cavity Equipped to a Hot Obstacle Using Nanofluids Considering Temperature-Dependent Properties, *International Journal of Heat and Mass Transfer, 85* (2015), June, pp. 656-666

[17] Aghaei, A., *et al*., Numerical Study of Magnetic Field on Mixed Convection and Entropy Generation of Nanofluid in a Trapezoidal Enclosure, *Journal of Magnetism and Magnetic Materials, 403* (2016), Apr., pp. 133-145

[18] Arefmanesh, A., *et al*., Mixed Convection Heat Transfer in a CuO-Water Filled Trapezoidal Enclosure, Effects of Various Constant and Variable Properties of the Nanofluid, *Applied Mathematical Modelling, 40*, (2016), 2, pp. 815-831

[19] Hussein, A., *et al*., Mixed Convection of Water-Based Nanofluids in a Rectangular Inclined Lid-Driven Cavity Partially Heated from its Left Side Wall, *Journal of Computational and Theoretical Nanoscience, 10*, (2013), 9, pp. 2222-2233

[20] Ahmed, S., *et al*., Mixed Convection from a Discrete Heat Source in Enclosures with Two Adjacent Moving Walls and Filled with Micropolar Nanofluids, *Engineering Science and Technology –- an International Journal, 19* (2016), 1, pp. 364-376

[21] Hemmat Esfe, M., *et al*., Heat Transfer Characteristics and Pressure Drop of COOH-Functionalized DWCNTs/Water Nanofluid in Turbulent Flow at Low Concentrations, *International Journal of Heat and Mass Transfer, 73* (2014), C, pp. 186-194

[22] Abdul Hakeem, A. K., *et al*., Buoyancy Convection in a Square Cavity with Mutually Orthogonal Heat Generating Baffles, *International Journal of Heat and Fluid Flow, 29* (2008), 4, pp. 1164-1173

[23] Kandaswamy, P., *et al*., Effect of Baffle-Cavity Ratios on Buoyancy Convection in a Cavity with Mutually Orthogonal Heated Baffles, *International Journal of Heat and Mass Transfer, 51* (2008), 7-8, pp. 1830-1837
[24] Famouri, M., Hooman, K., Entropy Generation for Natural Convection by Heated Partitions in a Cavity, *International Communications in Heat and Mass Transfer, 35* (2008), 4, pp. 492-502
[25] Tiwari, R. K., Das, M. K., Heat Transfer Augmentation in a Two-Sided Lid-Driven Differentially Heated Square Cavity Utilizing Nanofluids, *International Journal of Heat and Mass Transfer, 50* (2007), 9-10, pp. 2002-2018
[26] Abu-Nada, E., Chamkha, A. J., Mixed Convection Flow in a Lid-Driven Inclined Square Enclosure Filled with a Nanofluid, *European Journal of Mechanics B/Fluids, 29* (2010), 6, pp. 472-482

Paper submitted: February 25, 2016
Paper revised: August 9, 2016
Paper accepted: August 17, 2016